PHYSICAL REVIEW D **96,** 123005 (2017)

Magnetic field effects on the crust structure of neutron stars

B. Franzon[*]
Frankfurt Institute for Advanced Studies, Ruth-Moufang-1 60438, Frankfurt am Main, Germany

R. Negreiros[†]
Instituto de Física, Universidade Federal Fluminense, Avenue Galeao. Milton Tavares 24210346, Niteroi, Brazil

S. Schramm[‡]
Frankfurt Institute for Advanced Studies, Ruth-Moufang-1 60438, Frankfurt am Main, Germany
(Received 10 March 2017; published 13 December 2017)

We study the effects of high magnetic fields on the structure and on the geometry of the crust in neutron stars. We find that the crust geometry is substantially modified by the magnetic field inside the star. We build stationary and axis-symmetric magnetized stellar models by using well-known equations of state to describe the neutron star crust, namely, the Skyrme model for the inner crust and the Baym-Pethick-Sutherland equation of state for the outer crust. We show that the magnetic field has a dual role, contributing to the crust deformation via the electromagnetic interaction (manifested in this case as the Lorentz force) and by contributing to curvature due to the energy stored in it. We also study a direct consequence of the crust deformation due to the magnetic field: the thermal relaxation time. This quantity, which is of great importance to the thermal evolution of neutron stars, is sensitive to the crust properties, and, as such, we show that it may be strongly affected by the magnetic field.

DOI: 10.1103/PhysRevD.96.123005

I. INTRODUCTION

The density of matter varies enormously in neutron stars, from about the density of iron (7.86 g/cm^3) on the stellar surface to values higher than the nuclear saturation density in the stellar core [1,2]. In the absence of an exact theory of superdense matter, different theoretical models predict different equations of state (EoS) and compositions to describe neutron stars (NS). Furthermore, the structure of NSs can be divided into the surface, composed of ions and nonrelativistic electrons; the outer crust, where the ions form a solid Coulomb lattice at densities lower than the neutron drip density $n_{\rm drip} \sim 4.3 \times 10^{11}$ g/cm^3; the inner crust region beyond neutron drip density, where neutrons leak out of nuclei up to densities $\sim 10^{14}$ g/cm^3; and, finally, the core region, typically composed of electrons, protons, and neutrons forming a relativistic fluid. It is also in the core that exotic degrees of freedom such as hyperons [3–6], quark matter [7–11], and superconducting phases might appear [12–14].

With approximately 1 km in thickness, the crust region of neutron stars has an equation of state relatively well known; see Refs. [15–17]. In general, the composition, the structure, and the equation of state of the outer crust are determined by finding the ground state of cold ionic matter. In other words, this corresponds to minimizing the Gibbs energy per nucleon at a given pressure. In this case, one nucleus occupies a neutral unit Winger-Seitz cell, which together with the nucleus and the electrons contributes also to the total energy and pressure of the system. Here, we describe the ground state of matter in the outer crust of neutron stars by using the classical work formulated by Baym *et al.* [18].

The inner crust of neutron stars begins when neutrons start to drip out of the nuclei at densities about $n_{\rm drip}$. From this value to densities at the crust-core transition point, one has very neutron rich nuclei immersed in a gas of neutrons. In this case, the equation of state is usually obtained with many-body techniques such as Hartree-Fock, the Thomas Fermi approximation, and the compressible liquid drop model (CLDM). In this context, we follow the prescription of Ref. [19] to describe the structure and composition of the inner neutron star. The authors in Ref. [19] calculated the ground state of matter within the CLDM with Skyrme Lyon (SLy) effective nucleon-nucleon interaction. It is worth mentioning that other equations of state for this regime can be found in Refs. [20,21]. However, the choice of a particular EoS does not alter our conclusions. In addition, it is generally accepted that a pasta phase may appear in the crust-core transition [22–24]. Although the properties of the inner crust are modified in the presence of pasta phases, we do not take them into account in this work.

Because of its low-density regime, the crust has just a small contribution to the total mass in neutron stars [25]. Notwithstanding, the crust region is not only crucial not for

[*]franzon@fias.uni-frankfurt.de
[†]rnegreiros@id.uff.br
[‡]schramm@fias.uni-frankfurt.de

determining the stellar radius, which is of major present importance due to large uncertainties in the measurements of radii in NSs, but the crust also plays a crucial role in neutron star evolution, its dynamics, and observation. For example, the crust is related to phenomena such as glitches [26], the braking index [27], torsion modes [28–30], magnetic field evolution [31–33], thermal relaxation [34], and the cooling of neutron stars [35–37].

Certain classes of neutron stars are associated with very strong magnetic fields. According to observation of soft gamma-ray repeaters and anomalous x-ray pulsars, such stars show surface magnetic fields up to 10^{15} G [38,39]. These strong magnetic fields might be generated by dynamo processes in newly born neutron stars [40], although the exact origin of such high magnetic fields is still the subject of much debate. Moreover, according to the virial theorem, the magnetic field can reach values of $\sim 10^{18}$ G in the stellar core. According to Refs. [41,42], strong magnetic fields modify the equilibrium nuclear composition and the equation of state in neutron stars. However, as already shown in Refs. [43,44], the global properties of compact stars, such as the mass and the radius, do not change significantly with the inclusion of magnetic field effects in the equation of state of the dense matter. On the other hand, it was shown in Refs. [43,45] that the particle degrees of freedom at the core of stars change drastically with the inclusion of magnetic fields. Similarly, modifications of the crust properties and composition induced by magnetic fields can be seen in Refs. [46,47]. In this case, a more comprehensive study of the crustal EoS and its corresponding variation due to magnetic fields would be very desirable. However, it is to be noted that the inclusion of a crust magnetic field–dependent equation of state would require a consistent match with the magnetic field–dependent EoS of the core. Such analysis, however, requires much more insight into the microscopic of the crust, which is beyond the scope of this initial discussion of possible observable effects of magnetic fields in neutron stars.

Strong magnetic fields are also known to considerably change the structure of neutron stars. The authors in Refs. [43,44,48–50] evaluated magnetized models of stars endowed with strong poloidal magnetic fields. In this case, the Lorentz force induced by the magnetic field makes stars more massive, and they become oblate with respect to the symmetry axis. Moreover, effects of toroidal magnetic fields were addressed in Refs. [51,52]. In this case, the magnetized stars become more prolate with respect to the nonmagnetized case. Nonetheless, these works do not address the effects of strong magnetic fields on the global properties of the neutron star crust.

In this work, we construct equilibrium configurations of magnetized stellar models by using the same approach as in Refs. [48,53]. We make use of spherical polar coordinates (r, θ, ϕ) with origin at the stellar center and the pole located along the axis of symmetry. We focus on the size and geometry of the crust of highly deformed strongly magnetized neutron stars. In other words, we consider the different effects of the Lorentz force according to the angle and radius distribution inside the star.

The Lorentz force is related to the macroscopic currents that create the magnetic field, acting on the matter that can be pushed outward or inward. In the first case, we have the standard and expected effect of the Lorentz force, which acts against gravity, pushing the matter off center and making the star bigger on the equatorial plane and smaller at the pole. However, as we will see, the Lorentz force reverses direction inside the star, acting inward in the outer layers of the neutron star. It is important to note that, in addition to the Lorentz force just described, the magnetic field will also contribute to the curvature of space-time via the energy it stores. Note that once the spherical symmetry is broken in highly magnetized neutron stars the crust thickness depends on both the coordinate radius r and the angular direction θ.

The plan of the paper is as follows. In Sec. II we give a general overview of the Einstein-Maxwell equations that are required to be solved numerically. In Sec. III, we present our results for the crust thickness in strongly magnetized stars. Section IV contains our results for the thermal relaxation time of the stars discussed in Sec. III. Our final remarks and conclusions can be found in Sec. IV.

II. STELLAR MODELS WITH AXISYMMETRIC MAGNETIC FIELD

In this work, we construct models of stationary highly magnetized neutron stars. Details of the Einstein-Maxwell equations, numerical procedure, and tests can be found in Refs. [48,53]. We show here only the key equations that are solved numerically for the sake of completeness and better understanding for the reader.

Equilibrium stellar configuration are obtained in general relativity by solving the Einstein equations,

$$R_{\mu\nu} - \frac{1}{2} g_{\mu\nu} R = k T_{\mu\nu}, \tag{1}$$

with $R = g_{\mu\nu} R^{\mu\nu}$, $R_{\mu\nu}$ being the Ricci tensor, $g_{\mu\nu}$ being the metric tensor, k being a constant, and $T_{\mu\nu}$ being the energy-momentum tensor of the system. As we will be dealing with the macroscopic structure of neutron stars endowed with magnetic fields, the energy-momentum tensor of the system is given by

$$T_{\mu\nu} = (\mathcal{E} + P) u_\mu u_\nu + P g_{\mu\nu} + \frac{1}{\mu_0} \left(F_{\mu\alpha} F^{\alpha}_{\nu} - \frac{g_{\mu\nu}}{4} F_{\alpha\beta} F^{\alpha\beta} \right), \tag{2}$$

where the first term in Eq. (2) is the perfect fluid contribution, with the matter energy density $\mathcal{E}$, the isotropic fluid pressure P, and the 4-vector fluid velocity u_μ.

The second term represents the purely Maxwell stress tensor, with $F_{\alpha\beta}$ being the usual Faraday tensor defined in terms of the magnetic vector potential A_α as $F_{\alpha\beta} = \partial_\alpha A_\beta - \partial_\beta A_\alpha$.

According to Refs. [48,53,54], the metric tensor can be expressed in spherical-like coordinates (r, θ, ϕ) within the $3+1$ formalism as

$$ds^2 = -N^2 dt^2 + \Psi^2 r^2 \sin^2\theta (d\phi - N^\phi dt)^2 + \lambda^2 (dr^2 + r^2 d\theta^2), \quad (3)$$

with N, N^ϕ, Ψ, and λ being functions of the coordinates (r, θ). The equation of stationary motion $(\nabla_\mu T^{\mu\nu} = 0)$ for a perfect fluid with pure poloidal field can be expressed as [48]

$$H(r,\theta) + \nu(r,\theta) + M(r,\theta) = \text{const}, \quad (4)$$

where $H(r,\theta)$ is the logarithm of the dimensionless relativistic enthalpy per baryon, $\nu(r,\theta) = \ln N(r,\theta)$, and $M(r,\theta)$ is the dimensionless magnetic potential, which determines the magnetic field configuration,

$$M(r,\theta) = M(A_\phi(r,\theta)) := -\int_{A_\phi(r,\theta)}^{0} f(x)\mathrm{d}x, \quad (5)$$

with a current function $f(x)$ as defined in Ref. [53]. The Lorenz force induced by the magnetic field is proportional to $-\nabla M(r,\theta)$. Magnetic stellar configurations are determined by choosing a constant current function f_0. The magnetic field strength in the star increases proportionally with f_0. Moreover, the macroscopic electric current scale as $j^\phi = (\mathcal{E} + p) f_0$.

Note that the choice of a constant current function is the standard way to self-consistently generate a dipolar magnetic field throughout the star, in both the Newtownian and relativistic formalisms [55,56]. In addition, the effects of different current functions were already studied in Ref. [48]. They showed that several more complex distributions qualitatively generate the same magnetic field profile, even in the case in which there is no current in the center of the star (compare the dotted lines in the left panels of Figs. 11 and 15 in Ref. [48]). With respect to the quantitative differences, we explore them by changing the value of f_0. There are even more complicated current distributions that could, in principle, be used, but as shown by Ref. [48], they do not allow for numerical convergence due to the highly nonlinear character of Maxwell's equations.

III. CRUST THICKNESS OF STRONGLY MAGNETIZED STARS

We describe the inner crust with the Skyrme (Sky) EoS, which is based on the effective nuclear interaction SLy of the Skyrme type. For more details on the composition and EoS calculation, see Ref. [19]. The structure of the inner crust, and its EoS, was taken from Baym, Pethick, and Sutherland (BPS), based upon the Reid potential [18]. To describe the matter in the neutron star interior in the T = 0 approximation, we choose the Akmal-Pandharipande-Ravenhall EoS for the core [57], which is composed of protons, neutrons, electrons, and muons.

The equilibrium state of magnetized objects was discussed many years ago in Refs. [58,59]. More recently, many authors have shown that the stellar radius changes due to magnetic fields, where the star expands in the equatorial direction and contracts at the pole [43,44,48–50,53]. However, it is to be noted that the Lorentz force induced by magnetic fields reverses direction on the equatorial plane $(\theta = \pi/2)$ of the star [49] and might, therefore, impact the structure of the crust of neutron stars.

The crust thickness is defined as the difference between the stellar surface radius and the radius at the base of the crust where the crust-core transition takes place. As already calculated in Refs. [22,60], the symmetry energy affects the size of the inner crust considerably. In addition, in Ref. [61], the importance of a consistent matching between the core and the crust regions is shown. Although a more thorough study along this line would certainly be of interest, for the purposes of our studies, it is sufficient to use the the SLy and BPS results, for which the baryon number density at the crust-core transition is 0.076 fm^{-3}.

To illustrate the effects of strong magnetic fields on the neutron-star crust thickness, in Fig. 1, we show the crust thickness in the equatorial plane $(\theta = \pi/2)$, $\Delta r_{\rm eq}$, as a function of the central magnetic field, B_c, for stars at fixed baryon masses of $M_B = 1.40\,M_\odot$ and $M_B = 2.00\,M_\odot$, respectively. According to Fig. 1, the maximum magnetic field reached at the center of the star $M_B = 2.00\,M_\odot$ is 1.3×10^{18} G, while a star with $M_B = 1.40\,M_\odot$ has a central magnetic field of 0.9×10^{18} G. As one can see

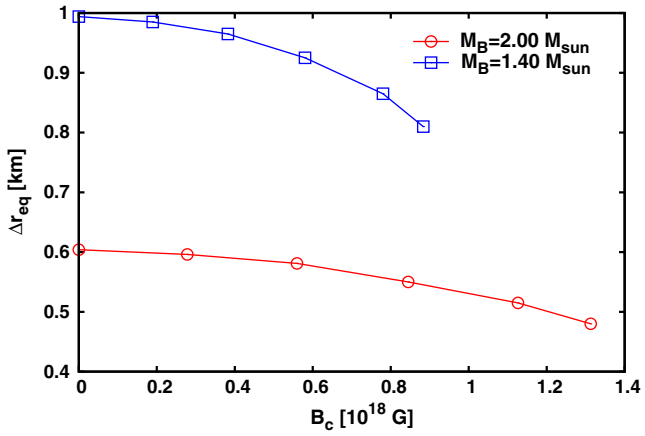

FIG. 1. Thickness of the crust $\Delta r_{\rm eq}$ in the equatorial plane $(\theta = \pi/2)$ as a function of central magnetic fields for stars at fixed baryon masses of $M_B = 1.40\,M_\odot$ and $M_B = 2.00\,M_\odot$.

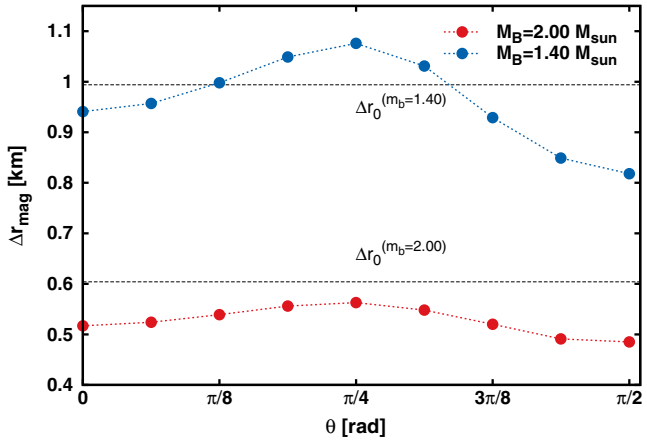

FIG. 2. Crust thickness $\Delta r_{\rm mag}$ in different angular directions θ for highly magnetized stars. These objects are the most magnetized stars as depicted in Fig. 1. For a star at a fixed baryon mass of $M_B = 1.40\,M_\odot$, the central magnetic field is $\sim 0.9 \times 10^{18}$ G, while $M_B = 2.00\,M_\odot$ has $\sim 1.3 \times 10^{18}$ G. The horizontal lines represent the crust thickness for spherical solutions (without magnetized fields), $\Delta r_0^{(1.40)} = 0.994$ km and $\Delta r_0^{(2.00)} = 0.604$ km for a star with $M_B = 1.40\,M_\odot$ and $M_B = 2.00\,M_\odot$, respectively.

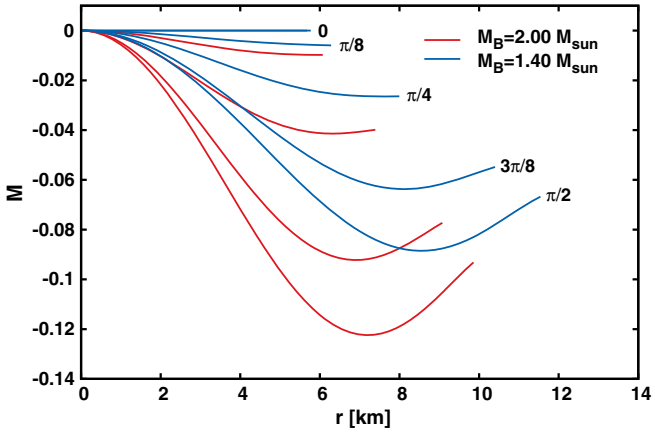

FIG. 3. Magnetic potential M as a function of the coordinate radius in different directions inside the stars. The corresponding stars are depicted in Fig. 2.

in Fig. 1, the crust thickness in the equatorial plane ia always reduced by the magnetic field. Note that stars with lower masses have a higher crust deformation. This is due to the fact that these stars have larger crusts extended over a larger radius and thus are *much* more easily deformed through the magnetic fields. On the other hand, for lower stellar mass, correspondingly lower magnetic field values are reached at the stellar center. This is because in a perfectly conducting fluid the magnetic field lines move with the fluid, i.e., the magnetic field lines are "frozen" into the plasma, and therefore the magnetic field strength is proportional to the local mass density of the fluid.

To study the effects of the Lorenz force on the crust of neutron stars, in Fig. 2, we show the crust thickness as a function of the polar angle θ for the most magnetized stars obtained in Fig. 1. We note that we have chosen the highest magnetic field configuration (i.e., the highest magnetic field before violating the virial theorem) so as to obtain an upper limit of the magnetic field effects on the crustal properties as well as the thermal relaxation of neutron stars. For smaller fields, the results found here will be qualitatively similar; however, the magnitude of the effect will be reduced, as the deformation of the star is also less pronounced for less magnetized stars. The horizontal lines in Fig. 2 correspond to the crust thickness for stars with baryon masses of $M_B = 1.40\,M_\odot$ and $M_B = 2.00\,M_\odot$, but without magnetic fields. In this case, the values for the crust thickness are $\Delta r_0^{(1.40)} = 0.994$ km and $\Delta r_0^{(2.00)} = 0.604$ km, respectively.

In Fig. 2, we depict stars that are deformed due to magnetic fields. As was already calculated in Refs. [48,49], the stellar configurations can strongly deviate from spherical symmetry due to the anisotropy of the energy-momentum tensor in the presence of strong magnetic fields. According to Fig. 2, the crust has a maximum expansion at $\theta = \pi/4$. For the less massive star ($M_B = 1.40\,M_\odot$), the crust expands and becomes larger than its nonmagnetized counterpart. From this point, the crust thickness is reduced. At the pole ($\theta = 0$), the Lorenz force is zero by symmetry (no electric current at the symmetry axis), but the crust thickness is smaller than in the nonmagnetized case. This is a geometric effect due to the expansion of the star on the equatorial plane. On the other hand, the increase of the crust thickness followed by a reduction at different polar angles is caused by the inversion of the direction of the Lorentz force inside the star.

To show the change of the Lorentz force according to its angular and radius distributions, in Fig. 3, we calculate the magnetic potential $M(r,\theta)$ as a function of the coordinate radius and at different polar angle directions for the same stars shown in Fig. 2. As a result, in Fig. 3, one observes that the magnetic potential presents a minimum at higher angles, for example, at $\theta = 3\pi/8$ and $\theta = \pi/2$ (for the star with $M_B = 1.40\,M_\odot$). These values correspond to angles for which the Lorentz force reverses sign and, as a consequence, changes its direction in the star. At lower polar angles, $M(r,\theta)$ decreases monotonically, and therefore the Lorenz force increases throughout the star, which leads to an expansion both of the inner and the outer layers of the star.

In Fig. 4, we show the size of the core for the same stars as those shown in Fig. 2 and Fig. 3. For a reference, we note that the radius (coordinate) of the core of an equivalent star with vanishing magnetic field is 8.41 km (for the $M_B = 2.00\,M_\odot$ star) and 9.38 km (for the $M_B = 1.40\,M_\odot$ star). The results in Fig. 4 indicate that highly magnetized stars expand their cores progressively from the pole ($\theta = 0$) to the equatorial plane ($\theta = \pi/2$) of the star. Note that the curves have an inflection point at $\theta = \pi/4$, which

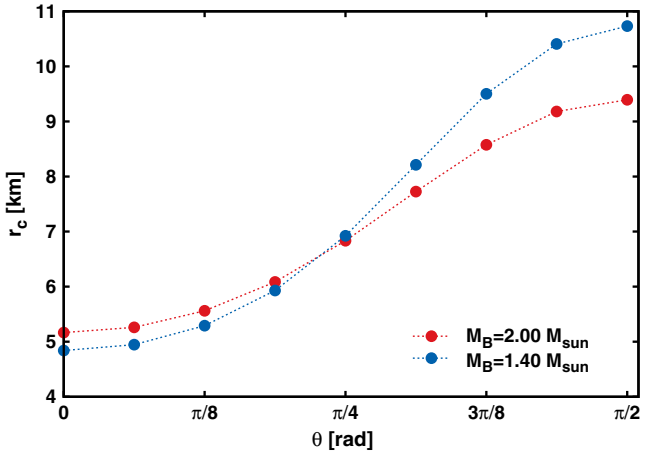

FIG. 4. Core thickness for the same stars as shown in Fig. 2.

corresponds to the angle where the Lorenz force reverses direction inside these stars. One must note, as discussed above, that, depending on the angle, the Lorentz force may act differently. For lower angles, since the Lorentz force decreases monotonically, it acts only repulsively, increasing both the core and the crust, whereas for higher angles, it has a minimum after which it acts attractively. Accordingly, for higher angles, one can see that the net effect of the Lorentz force on the core is repulsive (even though there is a small attractive region near the core-crust transition), which causes the core to expand for all angles in the presence of a magnetic field (albeit less intensively for higher angles). As for the crust, we find that for lower angles its size increases (as the Lorentz force is repulsive in these regions) but is reduced for higher angles (as the total effect of the Lorentz force in the crust is attractive for such angles).

Figure 5 depicts the physical quantities corresponding to the equation of motion in Eq. (4) as a function of the circular equatorial radius $R_{\rm circ}$ for a star with $M_B = 2.00\,M_\odot$. $R_{\rm circ}$ is defined as $R_{\rm circ} = \lambda(r_{\rm eq}, \pi/2) r_{\rm eq}$, with λ being the metric potential in Eq. (3) and $r_{\rm eq}$ being the coordinate equatorial radius. A detailed discussion about the coordinate system used in this work can be found in Ref. [53].

The upper plot in Fig. 5 represents a spherical and nonmagnetized stellar solution. The central plot shows the quantities from Eq. (4), i.e., C (= const), ν, M, and H, but taking into account magnetic fields. This is the same star as depicted in Figs. 2 and 4, respectively. In the bottom plot, we highlight the magnetic potential $M(r,\theta)$ and show the radii where the Lorentz force acts inward and outward inside the star. In all cases, the vertical lines represent the core-crust transition point and the stellar surface. As one can see, the star becomes bigger due to magnetic fields. However, the size of the crust decreases in the equatorial plane (see also Fig. 2).

For nonmagnetized stars, the magnetic potential is $M(r,\theta) = 0$. In addition, from Eq. (4), one has

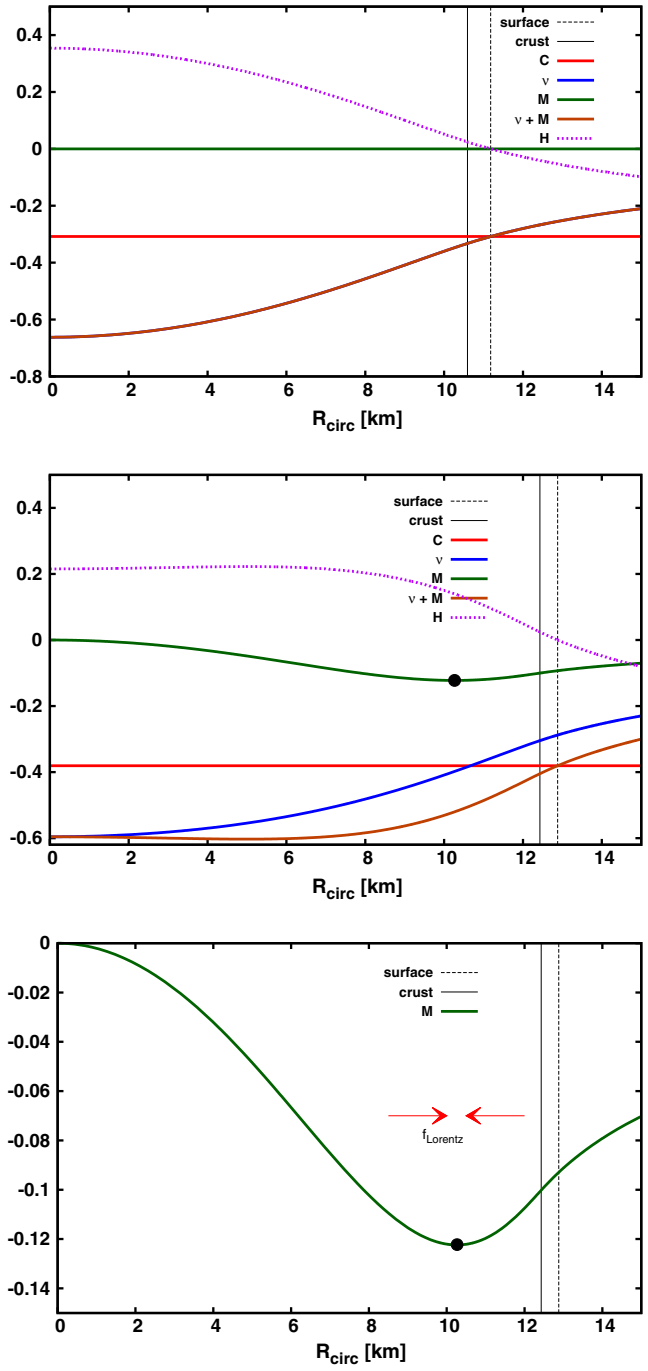

FIG. 5. Physical quantities presented in the equation of motion Eq. (4) as a function of the circular equatorial radius $R_{\rm circ}$ for a star with $M_B = 2.00 M_\odot$. The upper plot represents a spherical and nonmagnetized solution, and the middle figure shows the same star, but highly magnetized. The central magnetic field is 1.3×10^{18} G. We highlight the direction of the Lorentz force in the star in the lower panel. The vertical lines are the crust line and the stellar surface.

$H(r,\theta) + \nu(r,\theta) = \text{const} = C_0$. The constant C_0 can be calculated at any point in the star [49]. Since the input to construct the stellar models is given at the stellar center, we choose $C_0 = H(0,0) + \nu(0,0)$.

In the upper plot in Fig. 5, the surface of the star is found through the condition that the enthalpy goes to zero $H(r, \pi/2) = 0$, and therefore, from the equation of motion, Eq. (4), one gets $\nu = C_0$. In the magnetized case (center plot), we see that the enthalpy is reduced throughout the star and it reaches zero on the surface when $\nu + M = C_0$. An analysis similar to those described above was already performed before for neutron stars in Ref. [49] and for magnetized white dwarfs in Ref. [43].

The bottom plot in Fig. 5 shows the magnetic potential and the position and the direction (red arrows) of the Lorentz force inside the star. From the stellar center to the reversion point (black point), the Lorentz force acts outward, and therefore this part of the star expands. From the reversion to the crust-core radius (full black vertical line), the Lorentz force points inward. This also holds true for the region between the crust-core transition and the stellar surface (dashed black vertical line). As a result, the Lorentz force always points inward in the crust region, and therefore the crust is reduced in size. As a net effect, the star becomes bigger in the equatorial plane due to the increase of the core region.

IV. THERMAL RELAXATION OF MAGNETIZED NEUTRON STARS

The study and observation of the thermal evolution of neutron stars have been established as an important tool for probing the inner composition and structure of compact stars [62–67]. Many efforts have been dedicated toward a better comprehension of the thermal processes that may take place inside of neutron stars as well as the macroscopic structure effects that could affect the thermal evolution of such objects [67,68].

Most thermal evolution calculations are performed under the assumption of spherical symmetry and static structure composition, although efforts have been taken toward a self-consistent description of axis-symmetric neutron stars [68,69] and objects with a dynamic structure evolution [67]. The work in Ref. [68] shows that the thermal evolution of axis-symmetric neutron stars may be substantially different from that of spherically symmetric objects. Even though in the aforementioned paper the breaking of spherical symmetry is brought on due to rotation, it is reasonable to expect that a similar effect occurs if the spherical symmetry is broken due to the magnetic field as long as the resulting system also has an axis-symmetric structure.

A particularly interesting result, discussed in Ref. [68], is the modification of the core-crust coupling time in axis-symmetric neutron stars. The core-crust coupling time is given by the duration it takes for the core and the crust of neutron stars to become isothermal. Because of the difference in composition between the core (comprised of hadrons and leptons, and possibly of deconfined quark matter [66]) and the crust (mostly heavy ions in a crystalline structure and unbound neutrons in the inner crust), these two regions of the star have very distinct thermal properties, with substantially different neutrino emissivities, thermal conductivity, and specific heat [63]. Because of such differences, ordinarily the crust acts as a blanket, keeping the star's surface warm while the core cools down due to stronger neutrino emission. Eventually, the cold front, originating in the core, arrives at the crust, cooling it off as it moves to the surface. At this moment, a sudden drop in the stellar surface temperature is expected. Such a drop signals the moment in which the neutron star interior (core and crust) is thermalized. The magnitude of the temperature drop depends on whether or not fast cooling processes (mainly the Direct Urca process [62]) take place inside the neutron stars as well as how pervasive superfluidity/superconductivity is in the core. The presence of fast cooling processes would lead to a deeper and sharper surface temperature drop, whereas the absence of fast processes (slow cooling) affects a smoother drop in surface temperature. The core-crust coupling time, also referred to as the cooling relaxation time, has been studied extensively in Ref. [70], in which the authors find that the relaxation time, τ_w, may be written as

$$\tau_w = \alpha t_1, \tag{6}$$

where t_1 is a characteristic time that depends solely on crustal microscopic properties such as thermal conductivity and heat capacity. It is also sensitive to neutron pairing, which may be present in the crust. It is important to note that, as pointed out in Ref. [70], the constant t_1 is almost independent of the neutron star model. This is reasonable since, regardless of the uncertainties with respect to the high-density EoS, the composition of the crust is fairly known and understood. Note, however, that the work [70] did not consider the effects of magnetic fields on the microscopic properties of the crust, which could in principle affect t_1. We expect, however, that the inclusion of magnetic field effects on microscopic properties of the crust would primarily affect the thermal conductivity, as the low-mass electrons are more susceptible to magnetic field effects and are the prime agents in heat conduction in the crust. We believe that the magnetic field would introduce a direction dependence for the thermal conductivity, but it should not significantly change the magnitude of conductivity, which is most sensitive to the onset of neutron superfluidity in the crust. This quantity should remain mostly unchanged, since the magnetic field will have little effect on the neutron distribution. Furthermore, since in this work we are primarily concerned with the relaxation time of the whole crust and, thus, will be taking into account angular averaged quantities, as will become clear in the further sections, we expect that potential effects of the magnetic field on t_1 should not change our general conclusions. The constant α depends on stellar macroscopic properties and is given by

$$\alpha = \left(\frac{\Delta R}{1\ \mathrm{km}}\right)^2 \left(1 - \frac{r_g}{R}\right)^{-3/2}, \tag{7}$$

with ΔR being the crust thickness and where $r_g = 2GM/c^2$ is the gravitational radius, with M being the gravitational mass.

In Ref. [70], it is found that the neutron star relaxation time (t_w) scales with the size of the crust according to Eq. (6), more or less quickly, depending on how strong the superfluid effects are. Furthermore, it was also shown that the same conclusions hold for fast or slow cooling.

Given the results put forth in Refs. [70,68], in addition to the results we show in this work regarding the crust properties of magnetized neutron stars, it is only natural to consider how the magnetic field, and the changes it brings about, would affect the relaxation time. For this reason, we follow the study of Ref. [70] using the crust properties of magnetized neutron stars, as discussed in the sections above. One should note that the study presented here only establishes an upper limit for the thermal relaxation time for magnetized neutron stars. The reason for this is that, whereas the results in Ref. [70] were obtained for spherical symmetric stars, this is not the case for magnetized neutron stars that have a deformed axis-symmetric structure. In any case, the change in the crust thickness should allow us to make a reasonably good estimate of the relaxation time of such objects.

To estimate how the modification of the crust properties will affect the relaxation time, in Fig. 6, we consider the average crust thickness, $\Delta R = \sum \Delta r_{\mathrm{mag}}(\theta)/N_\theta$, as a function of the stellar magnetic field. In other words, the average ΔR is calculated for each value of the magnetic field, where $\Delta R_c(\theta)$ is the angular-dependent ($0 \leq \theta \leq 2\pi$) crust thickness and N_θ is the number of points in θ.

As Fig. 6 shows, the crust becomes, on average, thinner for moderately high magnetic fields and thicker for the larger values of B_s. In this context, thinner and thicker are to be

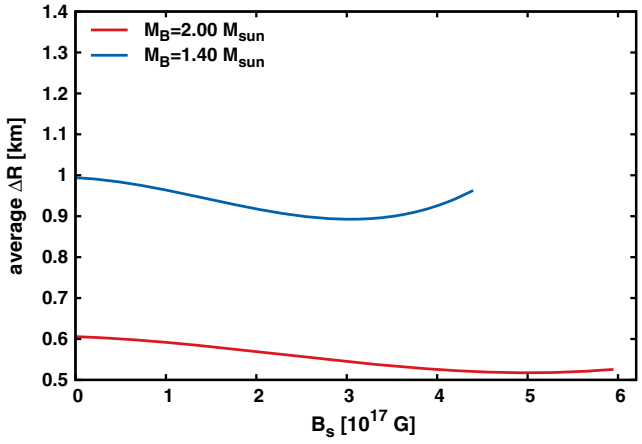

FIG. 6. Average crust thickness for different values of surface magnetic fields.

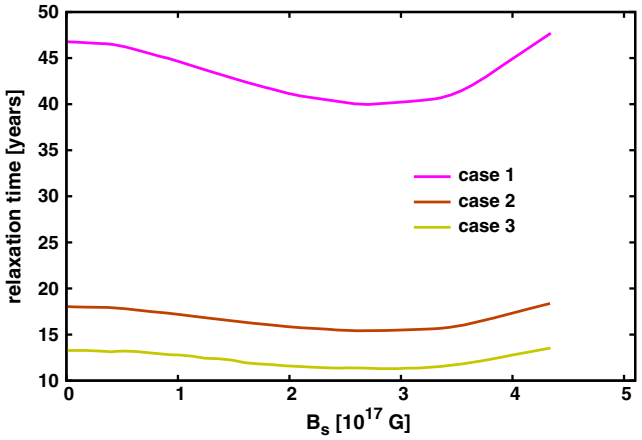

FIG. 7. Relaxation time for the $1.40 M_\odot$ star. The three curves indicate the three cases investigated, namely, $t_1 = 28.8$ yr (case 1), associated with absence of superfluidity in the crust; $t_1 = 11.1$ yr, associated with weak superfluidity in the crust (case 2); and $t_1 = 8.2$ yr for the case of strong crustal superfluidity (case 3).

considered with respect to those of an equivalent star with vanishing magnetic field. This is different than what happens in a(n) (also axially symmetric) rotating neutron star, the crust of which always gets thicker with the increase of the rotational frequency [68]. We believe that the reason for such a difference is connected to the Lorentz force induced by the current distribution inside the star. For the magnetic fields studied in this paper, the Lorentz force is attractive in the crust (same direction as the gravitational force), being stronger in the equatorial direction. This means that the crust will tend to become thinner on average for higher magnetic fields. On the other hand, one must note that the electromagnetic field in a general relativistic scenario has a dual role: it generates an electromagnetic force (in this case, in the form of the Lorentz force, as just discussed), and with the electromagnetic energy, it contributes to the curvature of space-time (see Refs. [71,72] and references therein for a more detailed discussion). Therefore, there are two competing effects: one tending to thin the crust and another causing it to be thicker (both on average). For moderately high magnetic field, the former one is stronger, and the crust becomes thinner (on average), whereas the latter is dominant for very high magnetic field, causing the crust to become thicker (also on average). Evidently, the star with $1.40\,M_\odot$, which has a lower gravity (i.e., curvature) is more susceptible to magnetic field effects and thus has a more pronounced effect, as illustrated in Fig. 6.

Following the steps of Ref. [70] and using the average crust thickness, we now estimate the upper limit for the relaxation time of magnetized neutron stars. For that, as in Ref. [70], we consider three situations, identified by three different values for the normalization constant t_1, namely, $t_1 = 28.8$ yr (case 1), associated with absence of superfluidity in the crust; $t_1 = 11.1$ yr, associated with weak

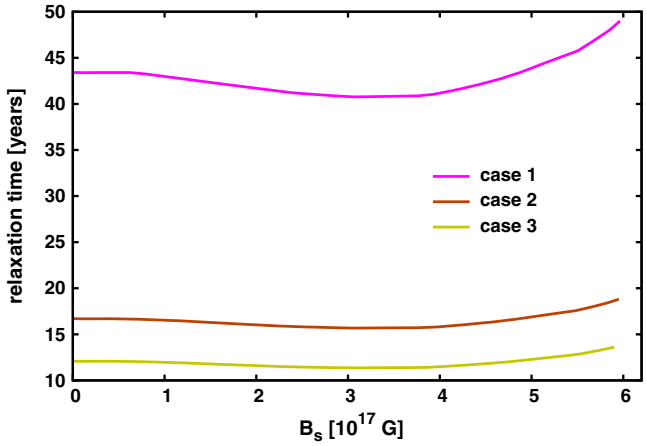

FIG. 8. Same as Fig. 7 but for the $2.0\,M_\odot$ star.

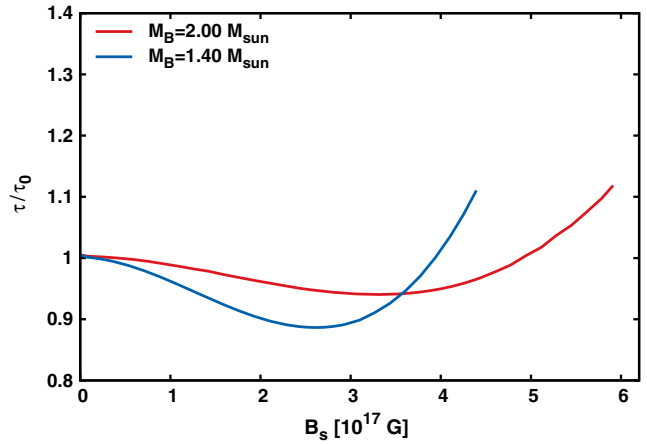

FIG. 9. Relaxation time normalized by the relaxation time of stars with vanishing magnetic fields, as a function of surface magnetic fields for star at 1.40 and $2.0\,M_\odot$.

superfluidity in the crust (case 2); and $t_1 = 8.2$ yr for the case of strong crustal superfluidity (case 3). The results are shown in Figs. 7 and 8 for the 1.40 and $2.0\,M_\odot$ stars, respectively.

As expected, due to quadratic dependence on the crust thickness, the relaxation time initially decreases as a function of the magnetic field and increases for higher values of B. Once again, the $1.40\,M_\odot$ star is more susceptible to the effects of the magnetic field.

If one wants to eliminate the uncertainties associated with the normalized time (t_1, which is connected to the extent and intensity of superfluidity in the crust), one can evaluate τ_w/τ_0, where τ_0 is the relaxation time for the case with $B_s = 0$. This result is shown in Fig. 9.

V. CONCLUSION

In this work, we studied strong poloidal magnetic fields effects on the global structure of the crust in stationary highly magnetized neutron stars. We self-consistently account for the Lorentz force, with current density bounded within the star, by solving the coupled equilibrium equations for magnetic and gravitational fields consistently, taking into account the stellar deformation due to anisotropies induced by magnetic fields. We have employed typical and well-known equations of state to describe the inner and the outer crust of neutron stars.

We found that the size of the crust changes according to its angular-dependent distribution inside the star. The magnetic force is zero along the symmetry axis, and its direction depends on the current distribution inside the star. Moreover, the magnetic field changes its direction, and therefore the Lorenz force reverses the direction inside the star. In our case, this can be seen from the change in behavior of the magnetic potential $M(r,\theta)$ around $\mathbf{R}_{\rm circ} \sim 10$ km in Fig. 5.

In this work, we have taken steps to estimate how the magnetic field and the consequent modification of the crust and space-time of the neutron star may affect the thermal evolution of neutron stars. In addition to the expected effects that a magnetic field may have on the microscopic composition, we have shown that the change in crust geometry may be very relevant to the overall cooling of neutron stars. Using the crust average thickness as a parameter, we estimated the upper limit for the thermal evolution relaxation time, which is the time scale for the core-crust thermal coupling. We have found that the crust thickness (on average), as a function of the quantity responsible for the breaking of spherical symmetry (the magnetic field in this case), gets smaller before growing. This is substantially different from other deformed axially symmetric neutron stars, such as rotating objects for instance. In the latter case, the crust gets always thicker as a function of the spherical symmetry breaking quantity (rotation/angular momentum in that case). We conclude that the reason for such behavior lies in the dual role of electromagnetic field in a general relativistic scenario, the energy of which contributes to curvature in addition to the electromagnetic traditional interaction. We have found that for the studied stars, there are two competing effects: one is the Lorentz force that tends to make the crust thinner, whereas the gravitational contribution of the magnetic field tends to make the crust thicker. For moderately high magnetic fields, the former wins, and the crust gets thinner on average, whereas for extreme values of B, the latter is dominant, making the crust thicker overall. This behavior is reflected in our estimates of the core-crust coupling time, which, as a function of the surface magnetic field, gets initially smaller and increases for higher values of B. Such a result is interesting, since one would be inclined to believe that the relaxation time would increase monotonically with B. Note that the overall geometry of the star becomes more oblate with the increase of B, so such an assumption would be reasonable. However, due to the Lorentz force acting on the crust, its size is reduced for moderate values of B.

Our results represent magnetostatic equilibrium conditions. The stability of these equilibria is beyond the scope of this initial discussion on the possible observable through the crust geometry in highly magnetized stars. Note that purely poloidal or purely toroidal magnetic field configurations undergo intrinsic instabilities related to their geometries [73–82]. In this context, several calculations have also shown that stable equilibrium configurations are obtained for magnetic fields composed of both a poloidal and a toroidal component [83–90]. However, these models considered a poloidal-dominated geometry, with the toroidal-to-poloidal-energy ratio restricted to less than 10%. As a result, we do not expect qualitative changes in our results with the inclusion of toroidal magnetic fields.

In addition, we obtained surface magnetic fields values above those observed so far in neutron stars. Nevertheless, according to the virial theorem, the magnetic fields reached at the center of neutron stars are expected to be as high as the magnetic field values found in this work. Although we have restricted our investigation to purely poloidal magnetic field, which is not the most general case, we have shown, in a fully general relativity way, that strong magnetic field significantly affects the crust geometry and its size. As a result, the thermal properties of these objects such as the cooling relaxation time are affected correspondingly.

Evidently, our calculations should be seen as an upper limit for the relaxation time, since full thermal evolution calculations such as in Ref. [68] would be necessary. In any case, the interesting behavior of the crust geometry warrants further investigation and shows that the thermal behavior of magnetized neutron stars may not be straightforward. Studies in which the magnetic field changes over time may lead to even more interesting and unexpected behavior. Current efforts are being made toward the investigation of different current distributions (which may lead to the Lorentz force having a different effect) as well as full two-dimensional thermal evolution calculation of magnetized neutron stars.

ACKNOWLEDGMENTS

B. F. acknowledges support from CNPq/Brazil, DAAD, and HGS-HIRe for FAIR. R. N. acknowledges the financial support from CAPES and CNPQ. R. N. also acknowledges that this work is a part of the project INCT-FNA Proc. No. 464898/2014-5. S. S. acknowledges support from the HIC for the FAIR LOEWE program. The authors wish to acknowledge the "NewCompStar" COST Action MP1304.

[1] F. Weber, *Pulsars as Astrophysical Laboratories for Nuclear and Particle Physics* (CRC Press, Boca Raton, FL, 1999).
[2] S. L. Shapiro and S. A. Teukolsky, *Black Holes, White Dwarfs and Neutron Stars: The Physics of Compact Objects* (Wiley, New York, 2008).
[3] N. Glendenning, Z. Phys. A **326**, 57 (1987).
[4] I. Bednarek, P. Haensel, J. Zdunik, M. Bejger, and R. Mańka, Astron. Astrophys. **543**, A157 (2012).
[5] I. Vidaña, Nucl. Phys. **A914**, 367 (2013).
[6] R. d. O. Gomes, V. Dexheimer, S. Schramm, and C. A. Z. Vasconcellos, Astrophys. J. **808**, 8 (2015).
[7] B. Franzon, D. A. Fogaca, F. S. Navarra, and J. E. Horvath, Phys. Rev. D **86**, 065031 (2012).
[8] F. Weber, J. Phys. G **25**, R195 (1999).
[9] M. Baldo, *Perspectives in Hadronic Physics* (Springer, New York, 2004), p. 189.
[10] M. Alford, D. Blaschke, A. Drago, T. Klähn, G. Pagliara, and J. Schaffner-Bielich, Nature (London) **445**, E7 (2007).
[11] B. Franzon, R. O. Gomes, and S. Schramm, Mon. Not. R. Astron. Soc. **463**, 571 (2016).
[12] M. Baldo, M. Buballa, G. Burgio, F. Neumann, M. Oertel, and H.-J. Schulze, Phys. Lett. B **562**, 153 (2003).
[13] D. B. Kaplan and S. Reddy, Phys. Rev. D **65**, 054042 (2002).
[14] G. Lugones and J. Horvath, Astron. Astrophys. **403**, 173 (2003).
[15] N. Chamel and P. Haensel, Living Rev. Relativity **11** (2008).
[16] C. Lorenz, D. Ravenhall, and C. Pethick, Phys. Rev. Lett. **70**, 379 (1993).
[17] J. Lattimer and M. Prakash, Astrophys. J. **550**, 426 (2001).
[18] G. Baym, C. Pethick, and P. Sutherland, Astrophys. J. **170**, 299 (1971).
[19] F. Douchin and P. Haensel, Astron. Astrophys. **380**, 151 (2001).
[20] J. Negele and D. Vautherin, Nucl. Phys. **A207**, 298 (1973).
[21] H. Shen, Phys. Rev. C **65**, 035802 (2002).
[22] F. Grill, H. Pais, C. Providência, I. Vidaña, and S. S. Avancini, Phys. Rev. C **90**, 045803 (2014).
[23] G. Watanabe, K. Iida, and K. Sato, Nucl. Phys. **A676**, 455 (2000).
[24] D. Ravenhall, C. Pethick, and J. Wilson, Phys. Rev. Lett. **50**, 2066 (1983).
[25] P. Haensel, *Physics of Neutron Star Interiors* (Springer, New York, 2001), p. 127.
[26] M. Ruderman, T. Zhu, and K. Chen, Astrophys. J. **492**, 267 (1998).
[27] K. Cheng, Y. Yuan, and J. Zhang, Astrophys. J. **564**, 909 (2002).
[28] Y. Levin and M. van Hoven, Mon. Not. R. Astron. Soc. **418**, 659 (2011).
[29] H. Sotani, K. Kokkotas, and N. Stergioulas, Mon. Not. R. Astron. Soc. **375**, 261 (2007).
[30] C. J. Hansen and D. F. Cioffi, Astrophys. J. **238**, 740 (1980).

[31] J. Pons and U. Geppert, Astron. Astrophys. **470**, 303 (2007).
[32] D. N. Aguilera, J. A. Pons, and J. A. Miralles, Astrophys. J. Lett. **673**, L167 (2008).
[33] A. Cumming, P. Arras, and E. Zweibel, Astrophys. J. **609**, 999 (2004).
[34] O. Y. Gnedin, D. G. Yakovlev, and A. Y. Potekhin, Mon. Not. R. Astron. Soc. **324**, 725 (2001).
[35] R. Negreiros, S. Schramm, and F. Weber, Phys. Rev. D **85**, 104019 (2012).
[36] C. O. Heinke and W. C. Ho, Astrophys. J. Lett. **719**, L167 (2010).
[37] D. Page, J. M. Lattimer, M. Prakash, and A. W. Steiner, Astrophys. J. **707**, 1131 (2009).
[38] G. Vasisht and E. Gotthelf, Astrophys. J. Lett. **486**, L129 (1997).
[39] C. Kouveliotou *et al.*, Nature (London) **393**, 235 (1998).
[40] C. Thompson and R. C. Duncan, Astrophys. J. **408**, 194 (1993).
[41] D. Lai and S. L. Shapiro, Astrophys. J. **383**, 745 (1991).
[42] S. Chakrabarty, D. Bandyopadhyay, and S. Pal, Phys. Rev. Lett. **78**, 2898 (1997).
[43] B. Franzon, V. Dexheimer, and S. Schramm, Mon. Not. R. Astron. Soc. **456**, 2937 (2016).
[44] D. Chatterjee, T. Elghozi, J. Novak, and M. Oertel, Mon. Not. R. Astron. Soc. **447**, 3785 (2015).
[45] B. Franzon, V. Dexheimer, and S. Schramm, Phys. Rev. D **94**, 044018 (2016).
[46] I.-S. Suh and G. Mathews, Astrophys. J. **546**, 1126 (2001).
[47] R. Nandi and D. Bandyopadhyay, J. Phys. Conf. Ser., **312**, 042016 (2011).
[48] M. Bocquet, S. Bonazzola, E. Gourgoulhon, and J. Novak, Astron. Astrophys. **301**, 757 (1995).
[49] C. Y. Cardall, M. Prakash, and J. M. Lattimer, Astrophys. J. **554**, 322 (2001).
[50] R. Mallick and S. Schramm, Phys. Rev. C **89**, 045805 (2014).
[51] J. Frieben and L. Rezzolla, Mon. Not. R. Astron. Soc. **427**, 3406 (2012).
[52] K. Kiuchi and K. Kotake, Mon. Not. R. Astron. Soc. **385**, 1327 (2008).
[53] S. Bonazzola, E. Gourgoulhon, M. Salgado, and J. Marck, Astron. Astrophys., **278**, 421 (1993).
[54] E. Gourgoulhon, *3+1 Formalism in General Relativity: Bases of Numerical Relativity* (Springer Science & Business Media, Berlin Springer Verlag, 2012), Vol. 846.
[55] S. Lander and D. Jones, Mon. Not. R. Astron. Soc. **395**, 2162 (2009).
[56] Y. Tomimura and Y. Eriguchi, Mon. Not. R. Astron. Soc. **359**, 1117 (2005).
[57] A. Akmal, V. Pandharipande, and D. Ravenhall, Phys. Rev. C **58**, 1804 (1998).
[58] V. Ferraro, Astrophys. J. **119**, 407 (1954).
[59] S. Chandrasekhar and K. H. Prendergast, Proc. Natl. Acad. Sci. U.S.A. **42**, 5 (1956).
[60] J. Xu, L.-W. Chen, B.-A. Li, and H.-R. Ma, Astrophys. J. **697**, 1549 (2009).
[61] M. Fortin, C. Providencia, A. Raduta, F. Gulminelli, J. Zdunik, P. Haensel, and M. Bejger, Phys. Rev. C **94**, 035804 (2016).
[62] D. Page, J. M. Lattimer, M. Prakash, and A. W. Steiner, Astrophys. J. Suppl. Ser. **155**, 623 (2004).
[63] D. Page, U. Geppert, and F. Weber, Nucl. Phys. **A777**, 497 (2006).
[64] D. Page, M. Prakash, J. M. Lattimer, and A. W. Steiner, Phys. Rev. Lett. **106**, 081101 (2011).
[65] R. Negreiros, V. A. Dexheimer, and S. Schramm, Phys. Rev. C **82**, 035803 (2010).
[66] R. Negreiros, V. a. Dexheimer, and S. Schramm, Phys. Rev. C **85**, 035805 (2012).
[67] R. Negreiros, S. Schramm, and F. Weber, Phys. Lett. B **718**, 1176 (2013).
[68] R. Negreiros, S. Schramm, and F. Weber, Phys. Rev. D **85**, 104019 (2012).
[69] D. N. Aguilera, J. A. Pons, and J. A. Miralles, Astron. Astrophys. **486**, 255 (2008).
[70] O. Y. Gnedin, D. G. Yakovlev, and A. Y. Potekhin, Mon. Not. R. Astron. Soc. **324**, 725 (2001).
[71] R. P. Negreiros, F. Weber, M. Malheiro, and V. Usov, Phys. Rev. D **80**, 083006 (2009).
[72] R. Picanço Negreiros, I. N. Mishustin, S. Schramm, and F. Weber, Phys. Rev. D **82**, 103010 (2010).
[73] P. Markey and R. Tayler, Mon. Not. R. Astron. Soc. **163**, 77 (1973).
[74] R. Tayler, Mon. Not. R. Astron. Soc. **161**, 365 (1973).
[75] G. Wright, Mon. Not. R. Astron. Soc. **162**, 339 (1973).
[76] E. Flowers and M. A. Ruderman, Astrophys. J. **215**, 302 (1977).
[77] S. K. Lander and D. Jones, Mon. Not. R. Astron. Soc. **424**, 482 (2012).
[78] J. Braithwaite, Astron. Astrophys. **453**, 687 (2006).
[79] R. Ciolfi and L. Rezzolla, Mon. Not. R. Astron. Soc. Lett. **435**, L43 (2013).
[80] P. D. Lasky, B. Zink, K. D. Kokkotas, and K. Glampedakis, Astrophys. J. Lett. **735**, L20 (2011).
[81] P. Marchant, A. Reisenegger, and T. Akgün, Mon. Not. R. Astron. Soc. **415**, 2426 (2011).
[82] J. Mitchell, J. Braithwaite, A. Reisenegger, H. Spruit, J. Valdivia, and N. Langer, Mon. Not. R. Astron. Soc. **447**, 1213 (2015).
[83] C. Armaza, A. Reisenegger, and J. A. Valdivia, Astrophys. J. **802**, 121 (2015).
[84] K. H. Prendergast, Astrophys. J. **123**, 498 (1956).
[85] J. Braithwaite and H. C. Spruit, Nature (London) **431**, 819 (2004).
[86] J. Braithwaite and Å. Nordlund, Astron. Astrophys. **450**, 1077 (2006).
[87] T. Akgün, A. Reisenegger, A. Mastrano, and P. Marchant, Mon. Not. R. Astron. Soc. **433**, 2445 (2013).
[88] S. Yoshida, S. Yoshida, and Y. Eriguchi, Astrophys. J. **651**, 462 (2006).
[89] K. Glampedakis, N. Andersson, and S. K. Lander, Mon. Not. R. Astron. Soc. **420**, 1263 (2012).
[90] R. Ciolfi, V. Ferrari, L. Gualtieri, and J. Pons, Mon. Not. R. Astron. Soc. **397**, 913 (2009).